# Application of a Source-Grid-Load-Storage Intelligent Fusion Terminal in Power Grid Dispatch Optimization

Siyang He[1], Jianhua Zhang[1,*], Weikai Rong[2], Xin Du[3], Guanglu He[1] and Yiliang Li[4]

[1]*State Grid Liaoning Electric Power Co., Ltd. Economic and Technology Research 1. Guizhou Power Grid Co., Ltd., du'yun, Guizhou, 558000, China*
[2]*Guizhou Power Grid Co., Ltd. Duyun Weng'an Power Supply Bureau, Qiannan Bouyei-Miaozu, Zizhizhou, Guizhou, 550400, China;*
[3]*Guizhou Power Grid Co., Ltd. Duyun Fuquan Power Supply Bureau, Fuquan, Guizhou, 550500, China*
[4]*Shang Hai Jiao Tong Uuniversity Si Chuan Research Institute, Chengdu, 610213, Sichuan, China*
*E-mail: zhangjh@im.gzdy.csg*
[*]*Corresponding Author*

Received 10 July 2025; Accepted 20 October 2025

## Abstract

With the large-scale integration of renewable energy into the power grid, uncertainty on both the supply and demand sides increases significantly. The traditional centralised dispatch model increasingly exposes limitations in real-time responsiveness, mitigating large fluctuations and accommodating intermittent wind and solar output of wind and solar power. Concurrently, increasingly complex load dynamics and the activation of distributed flexibility resources on the customer side have pose significant challenges to grid operations, including narrower regulatory margins, greater risks of

*Strategic Planning for Energy and the Environment, Vol. 45_1,* 47–76.
doi: 10.13052/spee1048-5236.4513

voltage deviations, and increased difficulties in achieving safe and economic coordination. This study proposes deploying edge-mounted intelligent fusion terminals that integrate power generation, transmission, load, and storage. These terminals are designed to enhance dispatch responsiveness and coordinated control under conditions of high renewable penetration. These terminals combine high-speed data acquisition, edge intelligent computing, and rapid collaborative control capabilities to aggregate multidimensional system-state information, perform millisecond-level device sensing, and generates real-time dispatch instructions through precise localisation and intelligent decision-making. Experimental validation under a representative scenario (20% daily renewable penetration and 30% peak-to-valley load difference) demonstrated significant performance improvements relative to a conventional dispatch system. The intelligent fusion terminals increased system adjustment speed by about 4.5 times, reduced load-tracking deviation by 78.2%, and improved ramping capability by over 70%, reducing required load shedding by up to 92%. Coordinated optimisation of storage charging/discharging and interruptible load response suppressed voltage fluctuations, maintaining the deviation rate within ±0.8% and increasing the voltage stability margin at critical nodes by 23%. In addition, average peak-hour network loss decreased by about 1.2 kW, renewable energy utilisation improved, and wind/solar curtailment fell by 23%. The collaborative optimisation model enabled by the intelligent fusion terminal offers a practical technical pathway toward a more resilient power grid and accelerated energy transition, demonstrating significant value for modern dispatch systems.

**Keywords:** Source-grid-load-storage collaborative optimization, intelligent fusion terminal, real-time power grid dispatch, renewable energy consumption.

## 1 Introduction

The global energy system is undergoing a rapid transition: large-scale integration of renewable generation – primarily wind and solar – into power systems is an accelerating and irreversible trend [1]. The inherent intermittency, volatility, and spatial dispersion characteristics of these resources pose unprecedented challenges for secure and economic grid operation [2, 3]. Consequently, the traditional scheduling paradigm relying on a centralized energy management system (EMS) faces increasingly severe limitations. Rising uncertainty on both the generation and demand sides significantly amplifies operational risk, and existing regulatory architecture cannot efficiently track the fast variations of renewable output and the complex, millisecond-to-second load dynamics that now occur in the system [4]. Meanwhile, the power system architecture is being fundamentally reconfigured: a proliferation of distributed resources on distribution networks and at the customer side has introduced substantial flexibility potential that must be actively harnessed to support reliability and economic operation.

In addition, the operational boundary of the power grid is becoming increasingly constrained: operating margins are narrowing, and issues such as voltage stability, frequency stability, and network congestion are increasingly intertwined and pronounced, while safety constraints grow more stringent [5]. Consequently, a centralized, hierarchical command-and-response dispatch paradigm is ill-suited to meet the stringent real-time coordination and performance requirements of systems with high renewable penetration. There is therefore an urgent need to explore new intelligent control approaches that provide enhanced situational awareness and edge autonomous collaboration [6, 7].

Driven by the "dual-carbon" goal, the emerging power system is characterized by high renewable energy penetration, stronger multi-directional load interactions, and an intensified need for coordinated operation among for source, grid, load, and storage. These trends create specific operational challenges. On the one hand, renewable energy sources such as wind power and photovoltaic power exhibit strong randomness and volatility. Their large-scale integration into the grid has reduced the system inertia and increased the challenges of stable voltage and frequency control. Consequently, the traditional thermal power-dominated scheduling approach struggles to adapt to the profound changes in the power supply structure. On the other hand, the explosive growth of interactive loads such as electric vehicles and distributed energy storage has transformed load characteristics from one-way stability to two-way fluctuations. The increased uncertainty in spatio-temporal distribution poses higher requirements for real-time response and accurate prediction capabilities. Moreover, achieving carbon-reduction objectives requires prioritizing renewable consumption without compromising supply reliability, which in turn calls for removing barriers among source, grid, load, and storage and implementing coordinated, multi-agent optimization across these elements.

As a core paradigm for ensuring the safe and efficient operation of the new power system, coordinated "source-grid-load-storage" interaction lies in breaking the information barriers and decision-making islands among source, grid, load, and storage, thereby enabling wide-area aggregation, flexible dispatch, and coordinated optimization of resources [8, 9]. However, efficient collaboration depends on an accurate and real-time perception system of global information and distributed collaborative control capabilities. Current architectures typically rely on independently deployed monitoring terminals and control devices that are single-purpose, based on heterogeneous data standards, and connected via complex communication protocols, which impedes coordination across links, regions, and time scales [10]. Centralizing all local data at a dispatch center further imposes heavy communication and computational burdens and degrades real-time decision-making due to transmission delay – especially for rapid fluctuations near the load or the end of the power supply [11]. Therefore, there is an urgent need for intelligent terminal equipment deployed at the grid edge that supports multi-dimensional data fusion, real-time edge decision-making, and efficient collaborative execution.

Traditional mathematical optimization algorithms (e.g., linear programming and dynamic programming) yield high accuracy and stable convergence for linear and small-scale problems but suffer from the curse of dimensionality and struggle to solve efficiently the multivariate, strongly coupled, and nonlinear problems in the "source-grid-load-storage" system. Heuristic algorithms, such as genetic algorithms and particle swarm optimization algorithms, offer strong global search capabilities for nonlinear, multi-constraint problems but typically exhibit slow convergence. Deep-learning-based intelligent algorithms possess strong self-learning and adaptive capabilities, which enabled them to accurately capture the dynamic behaviors and coupling relationships among the source, network, load, and storage. They are well suited in processing massive real-time data and supporting multi-objective collaborative optimization. These methods improve the adaptability of scheduling strategies through continuous iteration and satisfy the real-time, accuracy, and robustness requirements of intelligent fusion terminals. Consequently, deep-learning approaches have become the preferred solution for scheduling optimization; their ability to accommodate system complexity, perform multi-objective optimization, and learn dynamically allows full exploitation of intelligent fusion terminal capabilities and promotes overall optimization of power grid dispatch.

Intelligent converged terminal technology has emerged; its core value lies in deep integration of sensing, computing, communication, and execution functions into edge nodes. Deployment sites include grid connection points, critical transmission and distribution nodes, load aggregation points, and energy storage access points [12, 13]. These terminals enable millisecond-level collection, localized high-speed processing, and feature extraction of multidimensional information, including source output state, network topology, power flow distribution, load dynamic characteristics, storage charge and discharge state, and capabilities [14]. Crucially, the intelligent fusion terminal relies on its built-in edge intelligent computing engine to generate optimal control commands at the device or local-cluster level according to preset rules and local real-time constraints. It can also receive superior scheduling targets or boundary conditions without direct intervention from the scheduling center and execute closed-loop control actions within very short time frames [15]. This combination of "local self-consistency" and "regional collaboration", enabled by edge intelligence, establishes an efficient and agile control loop between core schedulers and massive end resources, which help bridge the gap between centralized optimization and decentralized control.

This study thoroughly explored the systematic value and implementation pathways of the "source-grid-load-storage" intelligent fusion terminals within power grid dispatching optimization framework. We analyzed the mechanisms by which these terminals enhance overall dispatching efficiency, delineated a novel, terminal-empowered scheduling architecture, and clarified the terminals' functional role in the closed loop of multi-time-scale collaborative scheduling. We further examined how high-quality and fine-grained local data acquired and generated by the terminals improved the accuracy and convergence performance of the optimization model, and how fast, local autonomous control strategy based on terminal edge decision-making served as a critical complement to wide-area optimal scheduling. Finally, we evaluated the effects of terminal information exchange and collaborative control mechanisms on the timeliness and reliability of scheduling instruction execution. The objective is to provide a rigorous theoretical foundation and practical guidance for developing next-generation power grid dispatching systems that better accommodate the energy transition and exhibit greater resilience, flexibility, and intelligence.

## 2 Theoretical Basis and Principle Technology

### 2.1 Optimization Theory of Power Grid Dispatching

The power grid consists of diverse decentralized distributed energy resources, including wind, solar, and fuel cells [16, 17]. As a new energy system, the distributed nature of the power grid presents substantial challenges for energy dispatching, which makes it a key research area.

Distributed energy dispatching aims at the allocation and utilization of energy to satisfy electricity demand. Typical objectives include maintaining system stability, reducing energy consumption and pollution, and maximizing energy efficiency [18]. Achieving these objectives requires an integrated set of techniques, including advanced energy management, storage, optimization, and grid coordination. In contrast to traditional power grids – where energy generation and consumption are relatively concentrated and dispatching is centrally governed – the distributed energy system features geographically dispersed generation and consumption across multiple nodes, which increases operational complexity of energy dispatch.

Distributed energy dispatching is a multi-objective optimization problem in the power grid, including cost reduction, efficiency improvement, and power supply uncertainty reduction [19, 20]. Centralized dispatching is increasingly inadequate to meet these requirements. Therefore, researchers have developed various algorithms, such as genetic algorithms, fuzzy logic control, and model predictive control, to achieve effective dispatching based on power grid conditions and energy availability and to optimize both energy utilization and economic performance.

The goal of power grid dispatching is to ensure reliable power delivery in an economical and environmentally sustainable manner by employing appropriate scheduling while minimizing operating costs [21]. This requires balancing operational expenses against environmental benefits to achieve a dispatch solution that is both cost-effective and environmentally compliant. Details are given in Equation (1).

$$C_{sum} = C_1 + C_2 \tag{1}$$

where $C_{sum}$ represents total cost, and $C_1$ represents operating costs, including fuel, maintenance, equipment depreciation, and power transaction expenses; $C_2$ denotes environmental costs, (i.e., pollution treatment expenses). The detailed expression for $C_1$ is given in Equation (2).

$$\begin{aligned} C_1 = \sum_{t=1}^{T}\sum_{i=1}^{N}\Bigg(&\Delta T C_i^{CG}(t) + \Delta T K_i P_i(t) + \sum_{i=1}^{N}\frac{ADC_i}{Pi_{i,max_i}} \\ &+ \sum_{t=1}^{T}\Delta T P_c(t) C_{grid}(t) + \sum_{t=1}^{T}\Delta T K_{bat}|P_{bat}(t)|\Bigg) \end{aligned} \tag{2}$$

where *T* represents the operation period of the power grid; *N* is the number of controllable units; $\Delta T$ is the time interval; $C_i^{CG}$ is the fuel cost per unit

$i$ in period $t$; $K_i$ is the maintenance cost of unit $i$; $P_i(t)$ is the output of unit $i$ in period $t$; $a$ is a constant; $ADC_i$ is the annual depreciation charge of unit $i$; $P_{i,max}$ is the maximum output power per unit *i*; $f_i$ is the capacity factor; $P_c(t)$ is the purchase and sale of electricity between the main power grid and the power grid in period $t$; $C_{grid}(t)$ is the cost of purchasing and selling electricity in period $t$; $P_{bat}(t)$ is the charge and discharge power of the battery in $t$ cycle; $K_{bat}$ is the battery charging and discharging cost. The environmental cost is given by Equation (3):

$$C_2 = \sum_{k=1}^{K} \alpha_k \lambda_{k1} P_{MT}(t) + \sum_{k=1}^{K} \alpha_k \lambda_{k2} P_{FC}(t) + \sum_{k=1}^{K} \alpha_k \lambda_{k3} CGP(t) \quad (3)$$

where $\alpha_k$ represents the external discount cost of *k*-type emissions; $\lambda_{kn}$ is the emission coefficient, which corresponds to *MT*, *FC*, and main grid, respectively; $K$ represents the type of emission; $P_{MT}(t)$ and $P_{FC}(t)$ represent the output power of *MT* and *FC* in period $t$, respectively; $CGP(t)$ denotes the purchasing power of the grid.

The battery capacity constraint $P_{SB}$ is defined by Equation (4).

$$-20 \leq P_{SB} \leq 20 \quad (4)$$

The charge/discharge limits of the battery are expressed by Equations (5)–(9).

$$P_{bat}(t) = P_{dis}(t) - P_{ch}(t) \quad (5)$$

$$0 \leq P_{dis}(t) \leq P_{dis}, max(t) \times U_{dis}(t) \quad (6)$$

$$0 \leq P_{ch}(t) \leq P_{ch}, max(t) \times U_{ch}(t) \quad (7)$$

$$U_{dis}(t) + U_{ch}(t) = 1 \quad (8)$$

$$\sum_{i=1}^{T} |U_{ch}(t) - U_{ch}(t-1)| \leq N_{bat} \quad (9)$$

The power $P_{bat}(t)$ of the battery at moment $t$ is obtained by subtracting the discharge power $P_{dis}(t)$ from the charging power $P_{ch}(t)$. The maximum discharge power is $P_{dis,max}(t)$, while the discharge state variable is $U_{dis}(t)$. Maximum charging power is $P_{ch,max}(t)$, while charging state variable is $U_{ch}(t)$. $T$ stands for transpose operation. The battery energy balance is limited by the initial and terminal stages, as expressed in Equation (10):

$$\sum_{i=1}^{T} P_{bat}(t) = 0 \tag{10}$$

where $P_{SB}$ is the output power of the battery, and $P_{dis}(t)$ and $P_{ch}(t)$ represent the discharge and charging power of the battery in $t$ cycle, respectively; $U_{dis}(t)$ and $U_{ch}(t)$ represent the state of the battery in $t$ cycle, with 1 being charged and 0 being discharged. $P_{dis,}max(t)$ is the maximum limit value of charge and discharge power of the battery in $t$ period; $N_{bat}$ is the maximum allowable value of battery charge and discharge times; $P_{bat}(t)$ is the sum of battery charge and discharge power.

The output constraints are expressed in Equation (11):

$$P_i, min(t) \leq P_i(t) \leq P_i,\ max(t) \tag{11}$$

The climbing speed is limited by the factors enumerated in Equation (12):

$$-R_i^{down}\Delta T \leq P_i^{CG}(t) - P_i^{CG}(t-1) \leq R_i^{up}\Delta T \tag{12}$$

where ***CG*** stands for the controllable unit power generation; $P_{i,min}^{CG}$ and $P_{i,max}^{CG}$ refer to the maximum and minimum outputs of the controllable unit $i$, respectively; $R_i^{down}$ and $R_i^{up}$ denote the descending and ascending climbing rates for unit $i$, respectively. The system constraints are expressed in Equation (13):

$$\sum_{i=1}^{N} P_i^{CG}(t) + \sum_{i=1}^{M} P_i^{RG}(t) + P_C(t) = P_L(t) \tag{13}$$

where ***RG*** represents the electricity generated by renewable power generation units; $P_i^{RG}(t)$ represents the output of ***RG*** cell $i$ in period $t$; $P_C(t)$ is the electricity purchased or sold by the power grid. $P_C(t) > 0$ indicates the sale of power to the main power grid, while $P_C(t) < 0$ indicates purchase of power from the main power grid; $P_L(t)$ denotes the grid system load.

## 2.2 "Source-grid-load-storage" collaborative operation mechanism

The large-scale integration of renewable energy into the grid has exposed limitations in the traditional real-time balancing paradigm, which are primarily

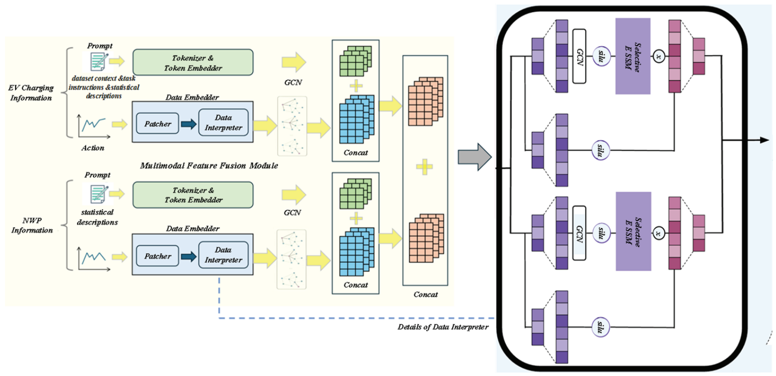


**Figure 1** Basic architecture of "source-network-load-storage" coordinated optimization.

due to inadequate adaptability to new energy equipment and insufficient grid operation flexibility [22]. The new power system emphasizes collaborative interactions among "source-grid-load-storage" and hierarchical cooperation between large power grid and microgrid. This approach enables a transition from real-time balancing toward non-real-time balancing mode and reinforces the role of renewable resources in system operation [23]. By integrating various resources and multiple optimization strategies, the "source-grid-load-storage" coordinated optimization promotes refined and intelligent management of the power system and serves as a key enabling technology to mitigate supply-demand imbalances caused by renewable integration. As the new power systems continue to develop, the "source-grid-load-storage" architecture will be crucial for optimizing resource allocation and improving energy utilization efficiency, thereby supporting sustainable development of power systems [24, 25]. Figure 1 presents the basic architecture.

The traditional fossil-fuel-based power system is transitioning to one dominated by renewable energy, in which wind, solar, and hydropower now constitute the primary generation sources, although some thermal power plants remain in operation [26]. Notably, the installed capacity of clean energy has surpassed that of traditional thermal power generation, marking a fundamental shift in the global energy mix.

The evolving energy structure has increased the strategic importance of the power grid [27]. The grid now encompasses local networks (e.g., microgrid distribution networks) and wider-area transmission networks, including high-voltage and ultra-high-voltage networks. In China, massive clean energy resources necessitate extensive cross-regional ultra-high voltage transmission and distribution networks. Meeting this demand requires reinforcing bulk-grid architecture to improve stability and integrating digital technologies to establish more digital infrastructure. Consequently, the power grid will evolve into a large-scale power system that can be deeply integrated with microgrids and distributed energy sources. This system forms a comprehensive, efficient, and intelligent energy transmission network that ensures reliable energy delivery.

Loads in power systems are conventionally classified as rigid and flexible. Rigid loads, such as critical industrial and public service facilities, exhibit fixed demand and are insensitive to electricity prices or incentive schemes. Flexible loads, such as household appliances, have temporally shiftable electricity consumption and can respond to electricity prices and incentive schemes, thereby realizing load transfer. End users can adjust operating schedules and on/off states to shift demand without compromising service quality or daily activities [28].

The increasing integration of renewable energy into the grid and the development of the electricity market make effective management of flexible loads essential for enhancing the efficiency and stability of the power system. It also contributes to promoting renewable energy utilization and the healthy development of the electricity market [29, 30]. Consequently, in-depth study of the roles of rigid and flexible loads in power system planning, design, operation, and management is of considerable academic and practical importance.

Energy storage technology plays a critical role in modern power systems. Energy storage smooths the load profile and therefore improves system stability and reliability by enabling temporal shifting and balancing of supply and demand. The increasing adoption of renewable energy sources, such as wind energy and solar energy, raises the variability and intermittency of power output, which complicates system operation and planning. Therefore, the efficient utilization of energy storage devices is essential to mitigate these challenges.

## 3 Development of a Scheduling Optimization Model Based on Intelligent Fusion Terminal

### 3.1 Incorporating the Response Characteristics of Intelligent Fusion Terminals Into the Scheduling Model

This study proposed a novel grid dispatching algorithm based on state decoupling adversarial training. The algorithm framework, presented in Figure 2,

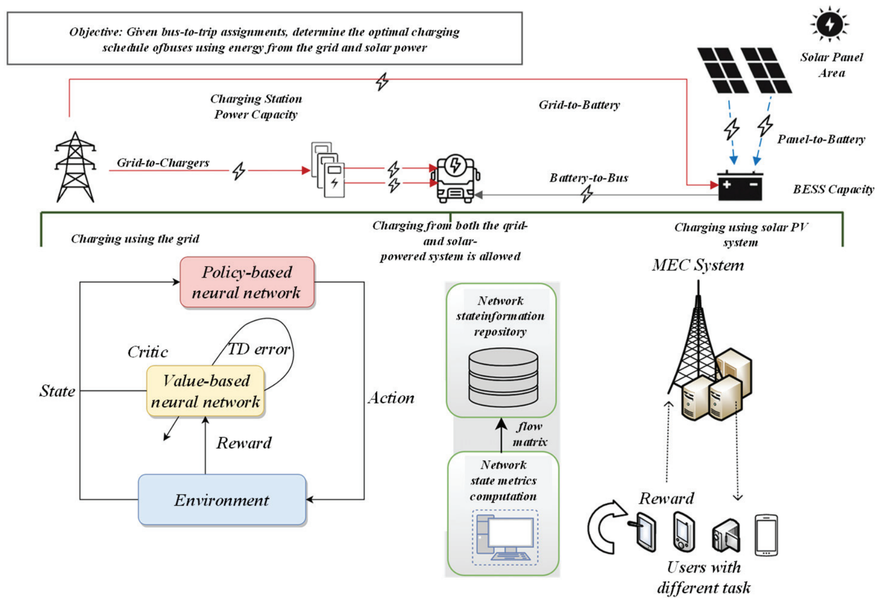


**Figure 2** Scheduling optimization model of response characteristics of intelligent fusion terminals.

comprises two complementary components: adversarial reinforcement learning and contrastive representation learning. In the adversarial reinforcement learning module, the uncertainty is modeled as a hostile agent, while the power grid dispatching agent serves as the principal agent for adversarial training. The hostile agent seeks to reduce the reward of the primary agent, while the primary agent develops a scheduling strategy to address uncertainty. The comparative representation learning module implements a state decoupling representation extraction that separates the environmental state along temporal and spatial dimensions. This mechanism produces stable state representation and therefore enhances the adversarial ability of the algorithm. For data collection, it acquires large volumes of accurate, real-time data from the power supply, grid, load, and energy storage subsystems, which constructs a dynamic data pool that provides a comprehensive, high-fidelity foundation for scheduling optimization. At the information interaction layer, the system functions as an "intelligent hub" that interfaces seamlessly with the equipment and dispatch centers across all links via standardized communication protocols. It aggregates, normalizes, and uploads distributed data, rapidly receives dispatch instructions, and accurately distributes them to the appropriate links. This approach eliminates information islands and ensures efficiency and consistent data transmission. For decision support, the system's embedded intelligent algorithm functions as a "brain center", which performs in-depth analysis and knowledge discovery on the collected multi-dimensional data and generates optimal dispatching schemes that account for grid operation constraints, load prediction, and new energy output characteristics. These recommendations enable dispatchers to make timely, evidence-based decisions that enhance the economic efficiency, safety, and reliability of the power grid.

In power-grid control applications, real-time disturbance-monitoring data (e.g., voltage fluctuations and sudden load-change signals) must be protected during transmission. We therefore encrypt such data at the edge using lightweight elliptic-curve cryptography algorithm (ECC) combined with an authenticated, dynamic key negotiation mechanism. Edge nodes adjust the key update frequency according to the disturbance level (sudden disturbance triggers instant key rotation) to prevent forgery of disturbance instructions after malicious data interception. When decomposing the state representation into real-time and historical information to optimize agent decision-making, historical records should be encrypted and stored using the national secret SM4 (SM4 Block Cipher) algorithm. Encryption keys must be securely provisioned and protected within a hardware security module (HSM) to prevent attackers from tampering with historical data and to ensure the integrity of decision-making model training.

The module consists of a front-end GTranXL for state representation and temporal decoupling and a back-end MLP. It must incorporate adversary-resilience mechanisms: both the real-time state (Xinstant) and historical state (Xchronics) are first passed through an anomaly detection layer based on an improved long short-term memory network (LSTM) to analyze temporal patterns and detect injected or corrupted state data. During normalization of location information, an identity mapping adjustment layer must integrate the hardware fingerprint generated by the terminal's physical unclonable function (PUF) to ensure that the state data source is trustworthy. Finally, a gating mechanism that enforces dynamic token verification is applied when reorganizing information, thereby preventing malicious modification of reorganization rules.

When extracting nonlinear information from the state representation by coupling the GTranXL module with the LSIM module, a zero-trust authentication mechanism is required to secure intermodule communication. To address the issue of increasing model complexity, we integrate a hash checking mechanism into the MLP dimensionality reduction layer downstream of GTranXL. This mechanism performs real-time checks on the computations and parameters of the dimensionality-reduction process and therefore prevents adversaries from introducing data noise via parameter tampering. The resulting low-dimensional state representation, when combined with encryption and additional anti-attack mechanisms, reduces noise and ensures data reliability, thereby improving the security of agent decision-making and the performance of grid dispatching.

Due to the instability of the training data and the high correlation between states, relying solely on the sparse rewards of reinforcement learning is insufficient to guide the learning of the representation extraction module. Consequently, additional unsupervised signal assistance is required to stabilize and improve the learning of state representations.

## 3.2 Function Positioning and Information Interaction Design of Intelligent Fusion Terminal in Scheduling Optimization

The hardware architecture of the proposed “source-grid-load-storage” intelligent fusion terminal is designed to support power grid scheduling by efficiently collecting and processing data across source, grid, load, and storage through accurate sensor selection, flexible communication module configuration, and systematic hardware unit construction. Sensor selection is driven by the requirements of specific physical quantity measurements. An AN1V series current sensor (Xinsen Electronics) is deployed for current monitoring on the source, charge, and storage sides. A high-precision Hall voltage sensor provides accurate voltage measurement. A PT100 temperature probe, a TE HTU31D temperature, and a humidity sensor (temperature accuracy $\pm 0.2°C$) are used to monitor equipment thermal conditions. An FR2V H00 series leakage current sensor is used for insulation monitoring of photovoltaic and energy storage DC links. A power sensor enables analysis of power distribution and flow direction. The communication module configuration employs a layered architecture, where the 4G/5G module facilitates long-range, high-speed data transmission in wireless communication, and the Wi-Fi module is well-suited for local area communication. Wired communication encompasses Ethernet modules utilizing TCP/IP protocols, RS-232/RS-485 serial port modules, and device interconnections facilitated by communication protocol conversion modules. The hardware architecture comprises a core processing unit, data acquisition unit, data storage unit, communication unit, human-computer interaction unit, power supply unit, and extended interface unit. This configuration provides solid hardware support for grid scheduling optimization.

The primary role of intelligent integrated terminals in the power grid dispatch optimization system is to combine an edge-perception center, a local decision-making node, and a collaborative execution unit. As the core interactive interface between the dispatching system and massive distributed resources, these terminals significantly improve the fidelity of multi-factor coupling models by accurately capturing operational characteristics across source, network, load, and storage. At the functional level, the terminal integrates high-precision synchronous measurement units and multi-protocol adaptation interfaces to achieve millisecond-level synchronous acquisition and dynamic feature extraction of multi-dimensional information (distributed power output characteristics), network (line power flow and node voltage), load (flexible load response characteristics), and storage (energy storage charging and discharging status) via cross-dimensional information association algorithms. These algorithms overcome the single-stream data limitations of traditional remote terminal units (RTUs) and smart meters. The terminal enables spatio-temporal unification and local fusion of cross-link and multi-type data by establishing a correlation mapping model for the real-time state of each element. This approach yields a time-sensitive and high-integrity global state information database that accurately represents the dynamic coupling relationship for upper-level scheduling optimization.

Based on embedded edge computing capabilities and lightweight artificial intelligence algorithms, the intelligent fusion terminal performs local, real-time computation and evaluation of key state variables to quantify: (1) the propagation effects of distributed power fluctuations on line loads; (2) the reverse impact of sudden load changes on energy storage charging/discharging strategies; and (3) the constraints that network limits impose on power output adjustments. The resulting coupling correlation features constitute an important supplementary input for the dispatch center's wide-area optimization model. The principal functional advance is a shift from passive data collection to active intelligent decision-making. According to the received superior scheduling targets, local real-time operation constraints, and a library of predefined optimization rules, the terminal independently generates optimal or near-optimal control strategies at the device or local-cluster level on local timescales by simulating the dynamic interactions among various elements. These strategies include the adjustment of the active/reactive power setpoints of the distributed power source, the release of energy storage charge and discharge power instructions, the generation of flexible load group aggregation response control signals, and the switching or gear adjustment of reactive power compensation devices. Commands are delivered directly to the local actuator via a high-speed control bus to form a closed-loop perception-decision-execution control. This local rapid decision-making capability effectively alleviates the dispatch center's real-time computational burden by explicitly accounting for the dynamic coupling among source, network, load, and storage, Particularly in wave suppression and safety correction scenarios that require rapid response, it significantly improves control timeliness and reliability.

To minimize the overall system cost, it is essential to account comprehensively for generation costs, energy storage charging/discharging losses, network losses, and compensation for load regulation actions. Cost-effective operation underpins the power system's sustainable development, and optimizing cost metrics therefore improve resource allocation efficiency and market competitiveness. Pursuing a high renewable-energy utilization rate aligns with the urgent structural transition required by the "dual carbon" strategy, and variability introduced by large shares of renewables must be absorbed through scheduling optimization to reduce renewable curtailment and facilitate clean-energy integration. Finally, maximizing power supply reliability (minimizing load reduction) is a fundamental obligation of the power system, which serves as a critical infrastructure that supports social production and daily life. Reducing the risk of power supply interruptions requires optimized operational scheduling and the explicit definition of constraints that delimit feasible and safe dispatch solutions. Power-balance constraints impose the power output, energy storage charging/discharging, load consumption, and network losses be balanced at every time step; this balance is a fundamental prerequisite for maintaining grid frequency stability. Equipment operational constraints specify the upper and lower output limits of distributed power sources, the charging/discharging power and capacity limits of energy storage, and the adjustment range of intelligent loads. These limits derive from the equipment's physical characteristics and the safety threshold and prevent damage or premature degradation from operating beyond safe bounds. Network constraints address transmission thermal limits and allowable voltage fluctuation ranges at nodes to prevent line overloads or voltage excursions that could compromise the secure and stable operation of the power grid.

At the information-interaction level, the intelligent fusion terminal implements a hierarchical, collaborative information interaction paradigm. In the downlink direction, the terminal establishes a reliable bidirectional communication channel with the dispatching center using standardized protocols. The terminal transmits not raw, voluminous data streams but distilled, high-value information produced by local preprocessing and feature extraction (e.g., key state quantities, local evaluation results, control execution feedback, and anomaly alerts). This edge processing significantly reduces the communication bandwidth requirements and the central data processing burden. Concurrently, the terminal receives the wide-area optimization target from the dispatching center, which serves as a boundary condition or optimization target reference for local decision-making. In the downlink direction, the terminal maintains a high-speed, low-latency control and information collection link with the source, network, load, and storage equipment controllers within its domain via local industrial Ethernet, the power line carrier or the wireless, private network, or other appropriate media. This connectivity enables rapid, precise command delivery and real-time aggregation of equipment status information.

To ensure the reliability and authenticity of the experimental data, the temporal and spatial scope of data collection was explicitly defined and documented. Temporally, the dataset spans up to 12 months and covers all four seasons, including peak electricity consumption periods, peak consumption periods, and special electricity consumption periods during holidays. The dataset captures seasonal and period-specific operational and load variations. Spatially, data were collected from diverse typical representative areas – such as urban core areas, suburbs, industrial parks, agricultural production regions, and remote mountainous regions – which correspond to different power consumption scenarios, such as high-density residential electricity, mixed electricity consumption at the urban-rural junction, high-energy-consuming industrial electricity, agricultural irrigation electricity, and decentralized remote user electricity consumption. All data were obtained from the power grid's operational real-time monitoring systems and historical databases.

The information interaction design of the intelligent fusion terminal emphasizes three principles: standardization, lightweight implementation, and security. A unified data model is adopted to ensure semantic interoperability between cross-link and cross-vendor devices. Message formats are kept lightweight and packet structures are optimized to minimize transmission delay. Simultaneously, high-level encryption authentication and access control mechanisms are integrated to ensure data confidentiality, integrity, and availability during both transmission and storage.

To address the limitations of simplified simulation scenarios, this study incorporates verification under complex operating conditions, including extreme weather events and sudden equipment failures. Extreme weather scenarios comprise strong typhoons, prolonged heavy rains, widespread high temperatures, and rare cold waves, which are used to assess impacts on new energy power generation efficiency, transmission line stability, and user electricity demand. Sudden fault scenarios include representative grid incidents such as abrupt transformer short circuits, single-phase grounding of transmission lines, and failures in the charging/discharging modules of energy storage systems. By constructing a simulation model of these complex scenarios, the scheduling optimization strategy of the "source-grid-load-storage" intelligent fusion terminal is tested in a harsh environment that more closely reflects actual power grid operation. This assessment validates the terminal's scheduling performance, robustness, and operational stability in responding to diverse severe contingencies.

### 3.3 Intelligent Integration of Endpoint Risks and Solutions

Communication latency degrades the timeliness and fidelity of real-time data of source, load, and storage received by the dispatch center. As a result, dispatching decisions based on delayed data may diverge from the actual operation state of the power grid. This situation may cause power imbalance, voltage fluctuations, and other problems that undermine system stability. Moreover, latency increases the response time of control terminals to sudden load changes or fluctuations in new energy output, degrades the execution efficiency of scheduling instructions, and can prevent the attainment of intended optimization objectives. To mitigate these risks, the following measures are recommended: (1) deploy advanced communication and distributed computing technologies (e.g., 5G and edge computing) to minimize transmission and processing delay and improve data timeliness; (2) establish continuous latency-monitoring and early-warning mechanisms that detect communication anomalies in real time and alert operators so that targeted corrective actions can be taken; (3) design delay-aware scheduling algorithms that explicitly account for communication delay and incorporate a delay compensation mechanism to improve the adaptability of the scheduling strategy to these delays.

## 4 Experiment and Result Analysis

To determine the optimal $\alpha$ value for the source-grid-load-storage intelligent fusion terminal scheduling optimization algorithm, $\alpha$ was varied from 0.1 to

0.9 in increments of 0.1. For each $\alpha$ value, the algorithm was trained 10 times. The average absolute percentage error (ARPE) of each training was recorded, and the mean ARPE across the ten trials was used as the performance metric. To verify the superiority of the proposed scheme, a quantitative comparative analysis of key indicators – including economic performance and reliability – was performed against an existing scheduling optimization scheme. From an economic standpoint, the existing scheme exhibited a mean ARPE of 8.5% across the evaluated operating conditions. The proposed method produced lower ARPE values throughout the tested range of $\alpha$. The mean ARPE attained its minimum value of 6.2% at $\alpha = 0.5$, which was 2.3% lower than that of the existing scheme (8.5%). This reduction corresponded to an approximately 27% decrease in economic loss associated with grid dispatch, which significantly improved the dispatching economy. In terms of reliability, the existing scheme exhibited an average power-supply interruption time of 12 min/month and a voltage-stability pass rate of 92%. When $\alpha = 0.5$, the proposed scheme reduced the average power supply interruption time to 5 minutes/month and increased the voltage stability pass rate to 98%. These results indicated that $\alpha = 0.5$ effectively improves the reliability of grid scheduling and reduces the power supply failure caused by scheduling problems. Figure 3 clearly showed that the ARPE value was the highest at $\alpha = 0.5$, and the corresponding scheme outperformed the existing scheme on key indicators. Therefore, the algorithm selects $\alpha = 0.5$ as the optimal parameter.

To verify the efficiency of the proposed wind power scenario clustering technology, which combines characteristic index dimensionality reduction with the analytic hierarchy process (AHP), we compared it against conventional K-means clustering technology. For the K-means algorithm, the optimal number of clusters was determined to be 6 using the DB index. The cluster center after iteration is depicted in Figure 4.

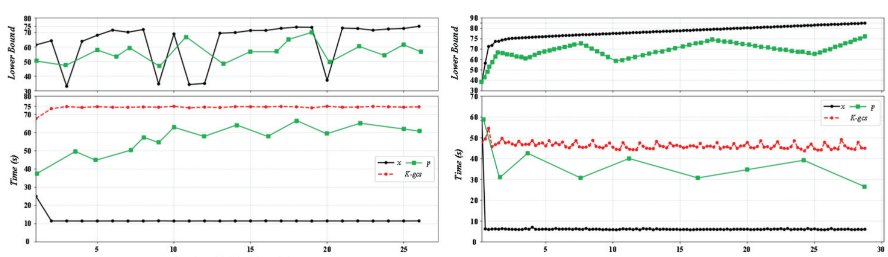


**Figure 3** Effect of different comparison loss weights $\alpha$ on algorithm performance.

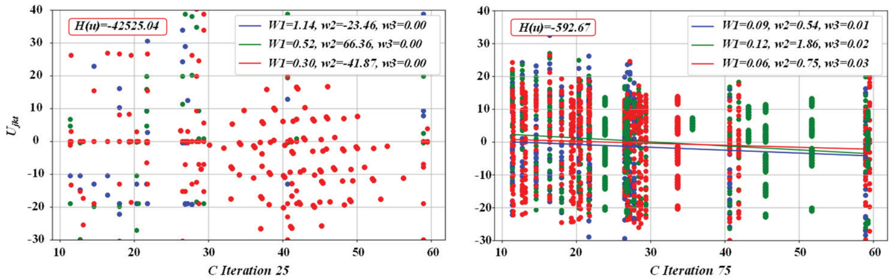


**Figure 4** Final clustering center.

**Table 1** DBI values for different numbers of clusters

| Number of Clusters | DBI Value | Number of Clusters | DBI Value |
|---|---|---|---|
| 3 | 0.85 | 8 | 1.18 |
| 4 | 1.50 | 9 | 1.04 |
| 5 | 1.56 | 10 | 0.83 |
| 6 | 1.24 | 11 | 0.95 |
| 7 | 1.11 | 12 | 0.88 |

We computed the DBI (Davies-Bouldin Index) values for different cluster counts, and the results are presented in Table 1. The DBI value attained its minimum at ten clusters, indicating the best clustering performance. Although three clusters yielded the second-lowest DBI, three scenarios were insufficient to develop a comprehensive peak shaving plan.

We computed each scenario's occurrence probability and its Kendall correlation coefficient with historical scenes. The results are presented in Figure 5. The summer scenario 1 and winter scenario 1 exhibited higher occurrence probabilities. This finding is consistent with the clustering results of the K-means algorithm. The Kendall correlation coefficients were generally high across the 10 typical scenarios, where the coefficients exceeded 0.9 for summer scenarios 1 and 2 and for winter scenario 1. These high correlations indicated that our algorithm can generate high-quality scenarios that truly reflect the wind power situation. The scenario occurrence probability is positively correlated with Kendall correlation coefficient, and the higher the scenario occurrence probability, the better the quality of scenes.

Figure 6 shows that the mixing loss exhibits some fluctuation in the early iterations but declines on the test set and stabilizes after 24 iterations. This behavior indicates that training simple predictors with the mixed-loss objective carries a low risk of overfitting.

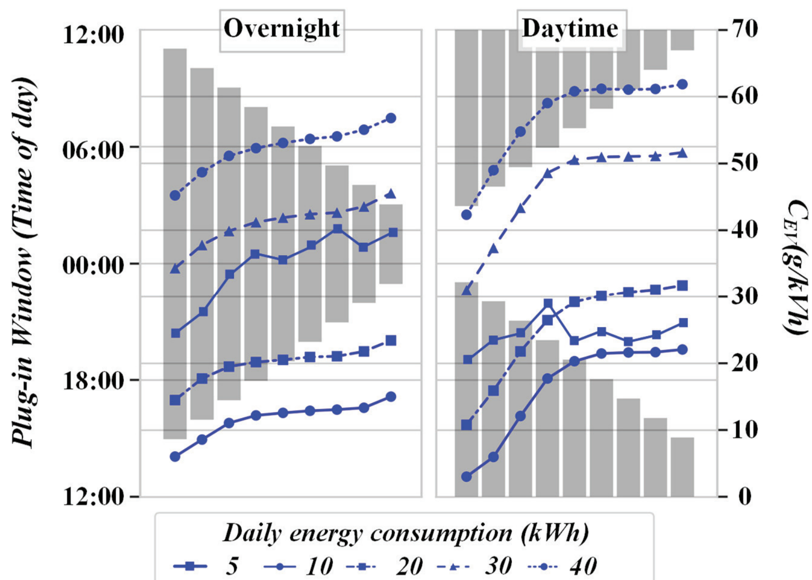


**Figure 5** Occurrence probability of various scenarios and their Kendall correlation coefficients with historical scenes.

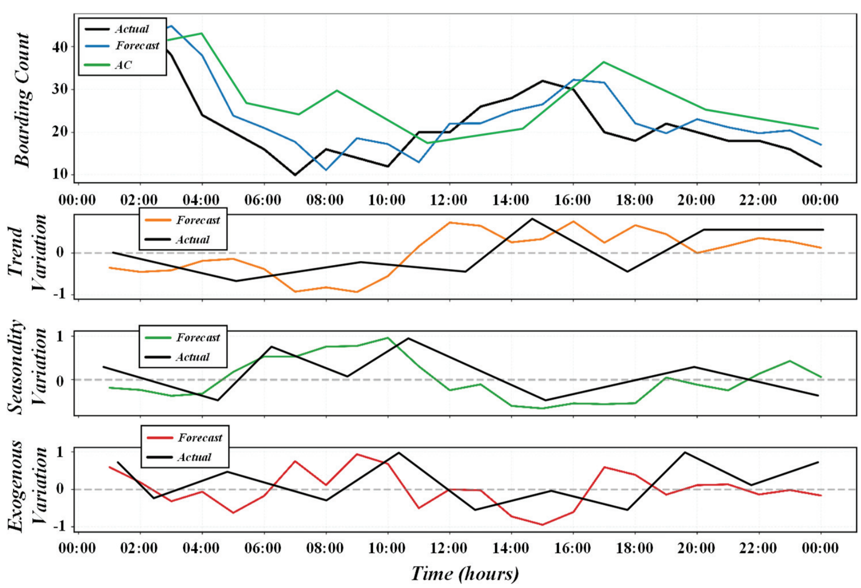


**Figure 6** Convergence of task loss across datasets.

**Table 2** Comparison of the mean performance of each method across all experiments

| Method | PICP (%) | | PINAW (%) | | CWC (Comprehensive Weighted Criterion) | |
|---|---|---|---|---|---|---|
| | PV1 | PV2 | PV1 | PV2 | PV1 | PV2 |
| M1 | 93.84 | 92.78 | 38.56 | 38.53 | 4.09 | 4.53 |
| M2 | 92.62 | 91.83 | 37.87 | 38.08 | 5.00 | 5.46 |
| M3 | 92.44 | 92.53 | 34.34 | 34.28 | 3.92 | 3.92 |

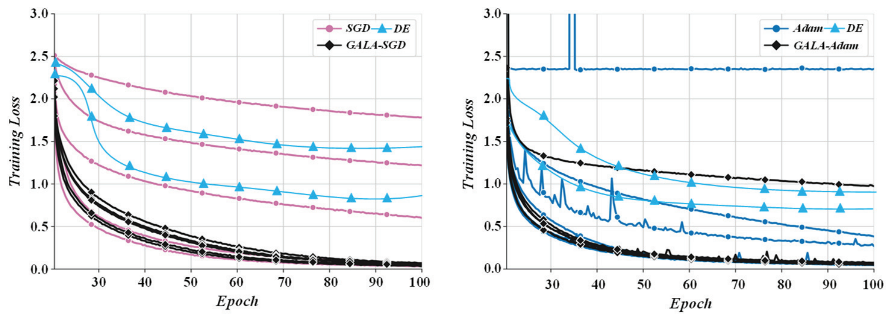


**Figure 7** Comparison of prediction results.

Table 2 summarizes the mean predicted performance metrics for the evaluated methods. The M3 method outperforms the control groups M2 and M3. The PICP (Prediction Interval Coverage Probability) reached 90% for all methods. The M3 method improved the PINAW (Prediction Interval Normalized Average Width) by about 4% relative to the other methods.

Figure 7 illustrates the output-power prediction results for the PV1 photovoltaic power plant using methods M1, M2, and M3. The prediction intervals produced by M3 were noticeably narrower than those of M1 and M2, which were similar to each other. These findings indicate that the proposed decision bias strategy effectively improves the prediction model's performance, leads to more concentrated prediction intervals, and positively impacts terminal decision-making optimization.

Table 3 summarizes the CWC metrics across all experiments and shows that M3 consistently achieves the best predictive performance. This result confirms the effectiveness of both the decision-bias strategy and the mixed-loss function in improving model prediction. The comparison between M3 and M1 shows that the mixed loss function significantly improves the performance. Although M2 and M3 were both pretrained from M1, M3's superior

**Table 3** Results for the comprehensive performance index CWC for each method across experiments

| | M1 | | M2 | | M3 | |
|---|---|---|---|---|---|---|
| Experiment Frequency | PV1 | PV2 | PV1 | PV2 | PV1 | PV2 |
| 1 | 4.07 | 4.09 | 4.05 | 4.10 | 3.88 | 3.92 |
| 2 | 4.15 | 4.10 | 4.14 | 4.07 | 3.98 | 3.98 |
| 3 | 4.13 | 4.08 | 4.13 | 4.09 | 3.97 | 3.92 |
| 4 | 4.10 | 4.11 | 4.04 | 9.06 | 3.91 | 3.90 |
| 5 | 4.12 | 4.11 | 4.05 | 4.11 | 3.93 | 3.91 |
| 6 | 4.10 | 8.48 | 8.83 | 8.54 | 3.92 | 3.92 |
| 7 | 4.07 | 4.04 | 8.54 | 4.03 | 3.90 | 3.91 |
| 8 | 4.07 | 4.17 | 4.07 | 8.44 | 3.95 | 3.92 |
| 9 | 3.99 | 4.04 | 4.02 | 4.05 | 3.86 | 3.85 |
| 10 | 4.10 | 4.09 | 4.06 | 4.08 | 3.94 | 3.98 |

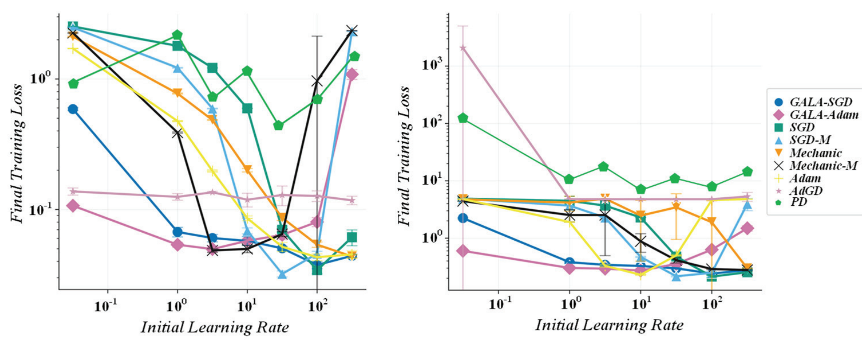


**Figure 8** Unit output results.

results demonstrated that the decision bias mechanism more effectively exploits the optimization information to improve the predictor.

Figure 8 indicates that wind curtailment occurred primarily during [1:00-8:00] and [19:00-24:00]. This pattern is mainly due to the frequent start-up and shutdown cycles of thermal power units, which increase operating costs. Consequently, wind curtailment was adopted to reduce overall operating expenses.

Table 4 compares the decision-making performance of the evaluated methods across different experimental scenarios. The decision bias quantifies the value of sample points, where scheduling cost represents system operating cost, and negative value represents profit. Overall, M3 demonstrated the best performance in both the decision bias and scheduling cost metrics.

**Table 4** SEM model fitness test

| Number of | Decision Bias | | | Scheduling Cost | | |
|---|---|---|---|---|---|---|
| Experiments | M1 | M2 | M3 | M1 | M2 | M3 |
| 1 | 0.215628 | 0.213996 | 0.123216 | −30.498 | −30.7938 | −35.0064 |
| 2 | 0.208896 | 0.208284 | 0.12087 | −30.5184 | −30.7836 | −34.4658 |
| 3 | 0.212262 | 0.210426 | 0.127092 | −30.549 | −30.8754 | −34.5678 |
| 4 | 0.20859 | 0.206346 | 0.129846 | −30.8448 | −31.1814 | −34.0068 |
| 5 | 0.217974 | 0.21675 | 0.124236 | −30.4776 | −30.702 | −34.5168 |
| 6 | 0.206754 | 0.20553 | 0.122604 | −31.2732 | −31.416 | −35.0574 |
| 7 | 0.19788 | 0.19533 | 0.121176 | −31.5384 | −31.9668 | −34.9248 |
| 8 | 0.22134 | 0.218076 | 0.123114 | −30.0492 | −30.447 | −34.3944 |
| 9 | 0.218994 | 0.216138 | 0.122502 | −29.886 | −30.3042 | −34.8942 |
| 10 | 0.205224 | 0.203286 | 0.124848 | −30.7428 | −31.0998 | −34.2108 |
| Avg. | 0.211344 | 0.209406 | 0.12393 | −30.6408 | −30.957 | −34.6086 |

## 5 Conclusions

This study examined the core role and key technology of "source-grid-load-storage" intelligent integrated terminals in modern power grid dispatching optimization. To address challenges arising from high penetration of distributed energy resources, such as volatility, increasingly complex power load, and urgent need for real-time regulation, the research deeply discussed the accurate perception of source information, real-time monitoring of network status, precise regulation of flexible loads, and the technology integration mechanisms and implementation pathways needed to enable intelligent decision-making by energy storage systems.

(1) Following integration of the terminal into collaborative optimization dispatch, the system's renewable energy consumption rate increased by 6.2%, thereby mitigating wind and solar curtailment and substantially improving the efficiency of clean energy utilization and the environmental performance of system operation.

(2) To assess its impact on the economic performance and operational security of the power grid, the converged terminal was validated using global coordination and optimization capabilities. The validation comprised joint optimization control of the voltages of 15 key nodes in the regional distribution network and online optimization of network losses. Following optimization, the voltage qualification rate at the regional key nodes rose from 97.5% to 99.2%, and the comprehensive network loss rate declined from 0.31% to 0.18%. These outcomes substantiated the

terminal's significant economic benefits in enhancing voltage stability and reducing network losses.

(3) A focused assessment was performed to evaluate the terminal's contribution to load-side response and energy storage synergy efficiency. The high-speed edge computing and wide-area communication capabilities of the converged terminal facilitated unified scheduling of large-scale distributed controllable loads. The aggregate response time was shortened to 3.1 seconds. In representative peak and off-peak scenarios, dynamic optimization of energy-storage charging/discharging strategies increased the average daily utilization rate of energy storage facilities by 11.7%. This improvement effectively exploited the huge peak shaving and valley filling potential of load elasticity and energy storage.

## Fundings

This work was supported by China Southern Power Grid Company Technology Project GZKJXM20240014.

## References

[1] H. Du, and X. Guo, "Cantor: A Novel Dynamic Source-Grid-Load-Storage Dispatching Model for Multiple Objectives in a Regional-Level Power System," LEEJ Transactions on Electrical and Electronic Engineering, vol. 20, no. 6, pp. 830–840, 2025. doi: 10.1002/tee.24246.

[2] H. Huang, Y. Li, and H. Liu, "Collaborative optimization strategy of source-grid-load-storage considering dynamic time series complementarity of multiple storages," let Generation Transmission & Distribution, vol. 17, no. 18, pp. 4007–4023, 2023. doi: 10.1049/gtd2.12862.

[3] Z. Lei, Q. Pei, J. Lian, J. Song, and Z. Zhang, "Research on optimal scheduling strategy of source-grid-load-storage in rural low-voltage distribution network," Archives of Electrical Engineering, vol. 73, no. 3, pp. 643–661, 2024. doi: 10.24425/aee.2024.150888.

[4] X. Huang, Y. Lin, X. Ruan, J. Li, and N. Cheng, "Smart grid energy scheduling based on improved dynamic programming algorithm and LSTM," Peerj Computer Science, vol. 9, 2023. doi: 10.7717/peerj-cs.1482.

[5] X. Li, J. Qian, C. Yang, B. Chen, X. Wang, Z. Jiang, and C.L. Bak, "New Power System Planning and Evolution Path with Multi-Flexibility

Resource Coordination," Energies, vol. 17, no. 1, 2024. doi: 10.3390/en 17010273.

[6] W. Qin, and J. He, "Research on adaptive dispatching of smart grid considering the cost of renewable energy power generation," International Journal of Global Energy Issues, vol. 46, no. 6, 2024. doi: 10.1504/ijgei.2024.141924.

[7] An, W., D. Ding, Z. Wang, Q. Liu and H. Dong, "Privacy-preserving distributed optimization for economic dispatch in smart grids," Automatica, vol. 177, pp. 112275, 2025. doi: 10.1016/j.automatica.2025.112275.

[8] Cai, Q., Y. Xu, Z. Yi, Z. Tu and H. Wang, "An improved two-stage robust optimization approach with adaptive uncertainty set for power system economic dispatch," Electric Power Systems Research, vol. 249, pp. 111957, 2025. doi: 10.1016/j.epsr.2025.111957.

[9] Cai, X., N. Zhang, L. Du-Ikonen and X. Lin, "Design a nationwide hydrogen grid: A GIS-based and iterative optimization model integrating pathfinding and dispatch," International Journal of Hydrogen Energy, vol. 154, pp. 150253, 2025. doi: 10.1016/j.ijhydene.2025.15 0253.

[10] Ces, N. P. L., J. B. Almada, F. L. Tofoli, R. F. Sampaio, L. S. Melo and R. P. S. Leão, "Comparative analysis of distributed optimization algorithms for economic dispatch in microgrids with energy storage systems," Journal of Energy Storage, vol. 132, pp. 117693, 2025. doi: 10.1016/j.est.2025.117693.

[11] Z. Li, Y. Yang, Y. Shi, L. Yao, W. Liu, and F. Wen, "Development of optimal participating strategy for source-grid-load-storage integrated projects in electricity markets with multi-stage joint optimization," let Renewable Power Generation, vol. 18, no. 16, pp. 4056–4068, 2024. doi: 10.1049/rpg2.13139.

[12] Y. Mi, Y. Chen, M. Yuan, Z. Li, B. Tao, and Y. Han, "Multi-Timescale Optimal Dispatching Strategy for Coordinated Source-Grid-Load-Storage Interaction in Active Distribution Networks Based on Second-Order Cone Planning," Energies, vol. 16, no. 3, 2023. doi: 10.3390/en16031356.

[13] Z. Shi, "Edge-end collaborative secure and rapid response method for multi-flow aggregated energy dispatch service in a distribution grid," Frontiers in Energy Research, vol. 12, 2024. doi: 10.3389/fenrg.2024.1 414511.

[14] B. Wang, Z. Tian, H. Yang, C. Li, X. Xu, S. Zhu, E. Du, and N. Zhang, "Collaborative Planning of Source-Grid-Load-Storage Considering

Wind and Photovoltaic Support Capabilities," Energies, vol. 18, no. 8, 2025. doi: 10.3390/en18082045.
[15] Y. Xu, S. Chen, K. Huang, C. Li, J. Liang, and G. Sun, "Pre-disaster distributionally robust scheduling model for active distribution networks considering topology reconfiguration, "Sustainable Energy Grids& Networks, vol. 43, 2025. doi: 10.1016/j.segan.2025.101725.
[16] Cheng, Y., G. Feng, S. Chang, Y. Liu and Y. Tang, "Research on dispatch strategy optimization of building micro-grid system in northeastern China," Solar Energy, vol. 300, pp. 113800, 2025. doi: 10.1016/j.so lener.2025.113800.
[17] Lee, Y., H. Choi, L. Pagnier, C. H. Kim, J. Lee, B. Jhun, H. Kim, J. Kurths and B. Kahng, "Reinforcement learning optimizes power dispatch in decentralized power grid," Chaos, Solitons & Fractals, vol. 186, pp. 115293, 2024. doi: 10.1016/j.chaos.2024.115293.
[18] Ma, A., Z. Li, F. Shen, X. Peng, Y. Liu, W. Zhong and F. Qian, "Multi-objective dispatch of integrated renewable power systems leveraging robust optimization in deep reinforcement learning," Computers & Chemical Engineering, vol. 201, pp. 109173, 2025. doi: 10.1016/j.co mpchemeng.2025.109173.
[19] H. Li, Q. Wu, L. Yang, H. Zhang, and S. Jiang, "Distributionally Robust Negative-Emission Optimal Energy Scheduling for Off-Grid Integrated Electricity-Heat Microgrid," Ieee Transactions on Sustainable Energy, vol. 15, no. 2, pp. 803–818, 2024. doi: 10.1109/tste.2023.3306360.
[20] F. Liu, Q. Mo, Y. Yang, P. Li, S. Wang, and Y. Xu, "A nonlinear model-based dynamic optimal scheduling of a grid-connected integrated energy system," Energy, vol. 243, 2022. doi: 10.1016/j.energy.2022.123115.
[21] D. Qi, X. Xi, Y. Tang, Y. Zheng, and Z. Guo, "Real-time scheduling of power grid digital twin tasks in cloud via deep reinforcement learning," Journal of Cloud Computing-Advances Systems and Applications, vol. 13, no. 1, 2024. doi: 10.1186/s13677-024-00683-z.
[22] Ma, Z., S. Wang, J. Shen, S. Li and Y. Shi, "Design of multi-energy joint optimization dispatching system for regional power grids based on B/S architecture," Energy Procedia, vol. 158, pp. 6236–6241, 2019. doi: 10.1016/j.egypro.2019.01.464.
[23] Meng, A., Z. Tan, H. Liu, Y. Huang, Y. Liu, G. Luo, J. Luo and H. Yin, "A bilateral secure economic dispatch model for wind-penetrated power systems using classification iteration optimization," Renewable Energy, vol. 249, pp. 123201, 2025. doi: 10.1016/j.renene.2025.123201.

[24] Sun, S., C. Wang, Y. Wang, X. Zhu and H. Lu, "Multi-objective optimization dispatching of a micro-grid considering uncertainty in wind power forecasting," Energy Reports, vol. 8, pp. 2859–2874, 2022. doi: 10.1016/j.egyr.2022.01.175.

[25] H. Qiu, W. Gu, C. Ning, X. Lu, P. Liu, and Z. Wu, "Multistage Mixed-Integer Robust Optimization for Power Grid Scheduling: An Efficient Reformulation Algorithm," LEEE Transactions on Sustainable Energy, vol. 14, no. 1, pp. 254–271, 2023. doi: 10.1109/tste.2022.3210214.

[26] B. Tang, J. Bao, N. Pan, M. Liu, J. Li, and Z. Xu, "Grid Operation and Inspection Resource Scheduling Based on an Adaptive Genetic Algorithm," International Journal of Engineering and Technology Innovation, vol. 14, no. 2, pp. 152–164, 2024. doi: 10.46604/ijeti.2024.13129.

[27] Z. Tong, Y. Zhou, and K. Xu, "An intelligent scheduling control method for smart grid based on deep learning," Mathematical Biosciences and Engineering, vol. 20, no. 5, pp. 7679–7695, 2023. doi: 10.3934/mbe.20 23331.

[28] Yin, L. and Y. Ye, "Distributed multi-objective African vulture accelerated optimization intelligent algorithm for multi-objective economic dispatch of power systems," Applied Energy, vol. 398, pp. 126377, 2025. doi: 10.1016/j.apenergy.2025.126377.

[29] Zhang, J. and Z. Hu, "Optimization study of county multi-level power grid co-dispatch based on hybrid game considering multivariate source-load interaction," Expert Systems with Applications, vol. 275, pp. 126981, 2025. doi: 10.1016/j.eswa.2025.126981.

[30] Zhang, M., W. Li, S. S. Yu, H. Li, Y. Lv and J. Shen, "A day-ahead self-dispatch optimization framework for load-side virtual control units participating in active power regulation of power grids," Energy, vol. 318, pp. 134791, 2025. doi: 10.1016/j.energy.2025.134791.

## Biographies

**Siyang He**

Senior Engineer

Academic qualifications: Master's degree candidate;

Has been engaged in the electrical engineering and automation profession for 18 years.

**Jianhua Zhang** graduated from North China Electric Power University (Beijing Campus). The work he participated in in August 2015. He has served as the director of the 500kV substation and the deputy general manager of the urban branch of the Duyun Power Supply Bureau of Guizhou Power Grid Company. His current position is the deputy general manager of the Production Technology Department of the Duyun Power Supply Bureau. He is familiar with the business of distribution grid production technology, and also has experience in main network work. He has good communication and coordination ability, production safety management ability and strong learning ability.

**Weikai Rong** (1995–);

Professional Title: Assistant engineer;

He is a member of the Communist Party of China. He has been engaged in seven years of work related to electrical engineering automation.

**Xin Du** (1997–);

Professional Title: Assistant engineer & Senior Workers;

He is a probationary member of the Communist Party of China. He has been engaged in low-voltage grid operation and maintenance and customer service for five years.

**Guanglu He** (1986–);

Professional Title: Engineer;

He is a member of the Chinese Communist Party. He has been majoring in power distribution operation for 10 years.

**Yiliang Li** (2000–);

He is a major in mechanical design, manufacturing and automation, and has been engaged in electricity-related majors for 1 year.